Thus, we have implemented a dynamics program making use of the CHARMM software, selecting an EF2 (improved empirical energy function) potential [5]. The individual trajectories were run for 4 ps after equilibration at 200 K. The crucial distance between the hydrogen in the ribose 2′-hydroxyl and the carbonyl oxygen in the uracil was monitored throughout the trajectories. Simultaneously, the puckering phase was also monitored. The resulting plots are displayed in Fig. 2a. The results should be contrasted with an analogous plot obtained after the proton has been transferred to the uracil. This last plot is displayed in Fig. 2b. The results can be interpreted as follows: In the initial situation, the distance lies within the range of an H bond in both free-energy minima for the sugar. In the C3′-endo pucker, the phase is in the range 20 – 55° and the distance remains within the H bond range. A similar situation is observed for the C2′-endo configuration, which, according to Fig. 2a, should be stabilized at 130 – 165°. We notice that in both configurations the possibility of proton transfer and consequently, of activation of the 2′-hydroxyl, is very high since the distance is in the range 1.9 – 2.7 Å. Moreover, a transition from one configuration to another always occurs concomitantly with a deactivation of the hydroxyl since, at intermediate configurations, the distance is higher than 2.7 Å. On the other hand, a direct inspection of Fig. 2b indicates that, after the proton transfer event has occurred, the stable configurations in the sugar are not correlated with any definite range in distance. Moreover, the ribose is far less locked into the most stable configurations, perhaps suggesting that an H bond does exist in the situation depicted in Fig. 2a. We can safely conclude that the 2′-hydroxyl has been deactivated after the proton transfer event.

Conversations with Manfred Eigen proved useful.

Received June 19, 1989

1. Krumhansl, J.A., Schrieffer, J.R.: Phys. Rev. B *11*, 3535 (1975)
2. Englander, S.W., Kallenbach, N.R., Heeger, A.J., Krumhansl, J.A., Litwin, S.: Proc. Nat. Acad. Sci. USA *77*, 7222 (1980)
3. Pace, N.R., Marsh, T.L.: Origins Life *16*, 97 (1985)
4. Fernández, A.: Naturwissenschaften *76*, 69 (1989)
5. Nilsson, L., Karplus, M.: J. Comp. Chem. *7*, 591 (1986)

Naturwissenschaften 76, 471 – 473 (1989)

The Fractal Nature of RNA Secondary Structure

M. D. Purugganan
Botany Department, University of Georgia, Athens, Georgia 30602, USA

The secondary structure of RNA is vital to the function of this molecule in biological systems. Recent theoretical [1] and experimental [2] advances have allowed workers to probe RNA folding patterns and correlate these with biological activity. Biophysical studies have demonstrated that many medium- to large-sized RNAs such as ribosomal [3, 4] and viral RNAs [5] exhibit a high degree of structural complexity. In these cases, RNA structure consists largely of helical stem-loop regions connected by single-stranded nucleotide segments, several of which may be hierarchically organized into discrete structural domains by long-range base-pairing. Studying the organization of these complex structures may prove useful in understanding the origin and evolution of these intricate assemblies, and their relation to RNA's functional roles.

Fractal geometry, which was first described by Mandelbrot [6, 7] has been applied fruitfully to the investigation of properties of irregular structures and processes. Fractals are structures possessing scale symmetry and scale invariance, and characterized by a fractal dimension, d_f. The fractal dimension is a real number which may differ from the Euclidean dimension of the embedding metric space. Physicists and chemists have applied the concepts of fractal geometry to explore such diverse phenomena as diffusion-limited aggregation, viscous fingering and surface chemistry [8]. Among biological macromolecules, the surfaces and backbone organization of proteins have been classified as fractal structures [9], and it has been suggested that the fractality of protein surfaces correlates with their biological binding properties. The Cantor fractal dust and its statistical equivalents [6, 10] are a class of fractals that describe hierarchical clustering, similar to that in the organization of secondary structure in RNA. The lengths of the clusters in Cantor and Cantor-like fractals follow an inverse hyperbolic distribution, such that

$$Pr(l) \sim l^{-d_f} \quad (1)$$

where $Pr(l)$ is the number of clusters with lengths greater than length l, and d_f is the fractal dimension, which ranges from zero to one.

The structural organization of several RNAs was studied in the context of the Cantor fractal set to investigate the extent of fractal clustering in RNA secondary structure. Previously determined RNA secondary structures were compiled from the literature [3 – 5, 11 – 15]. The statistical nature of the analyses precluded the use of small RNAs with known structures, and most of the structures used in this study were proposed on the basis of RNAse digestion experiments, computer predictions and/or phylogenetic comparisons.

Domain lengths of each RNA were determined by systematically decomposing the global folding pattern, as illustrated schematically in Fig. 1. The lengths of each structural unit were defined as being the number of residues between the terminal 5′ and 3′ base-paired nucleotides of each unit. The frequency of occurrence of structural units of length l for each RNA molecule

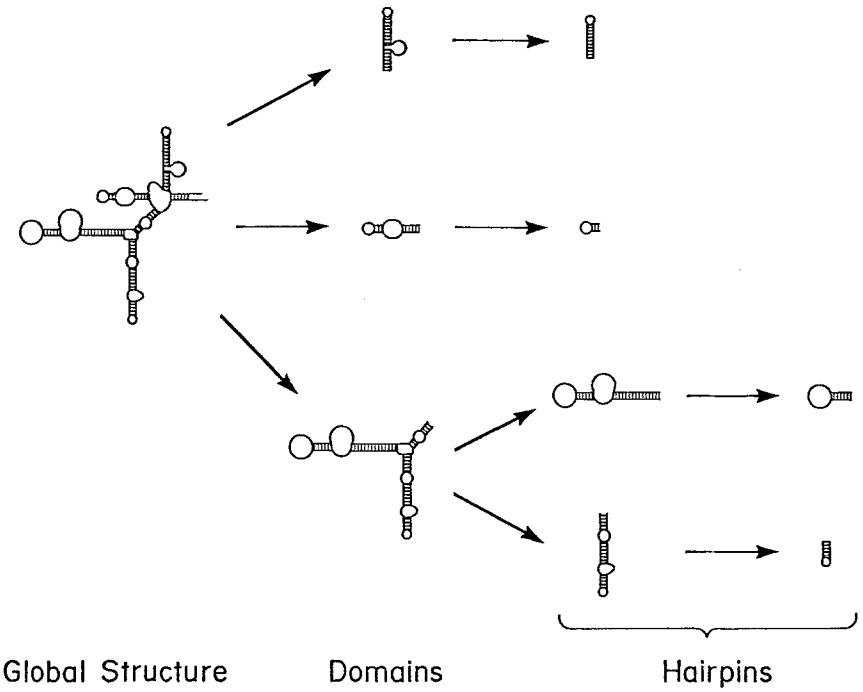

Fig. 1. Decomposition of global RNA secondary structure into component structural domains and hairpins. Single-stranded nucleotide segments are junctions that demarcate individual structures

was determined, and plotted as log $Pr(l)$ vs. log l, as defined in Eq. (1). A linear regression analysis was employed to determine d_f from the slopes of the distribution plots. To exclude finite boundary effects, the analysis was confined to the length ranges indicated in Table 1.

In the RNAs studied, structural clustering results in a distribution of lengths that conforms to the model for a Cantor-like fractal. Figure 2 shows plots of the inverse hyperbolic length distributions for several representative RNAs, and the calculated fractal dimensions are summarized in Table 1. The fractal dimension for RNA secondary structure ranges from 0.32 to 0.99, the average dimension being 0.69. As a reference, the triadic Cantor set has a dimension of 0.63.

Higher fractal dimensions are usually associated with a greater degree of embedded clustering, while low fractal dimensions correspond to a more gradual variation in structure sizes over a length range. Interestingly, the results suggest that the fractal dimensions of RNA secondary structure decreases in the order: viral RNA > RNAse P ≈ large subunit rRNA > small subunit rRNA > messenger RNA. Higher fractal dimensions are found in RNAs whose proposed secondary structures are necessary for their function. In the case of RNAse P and ribosomal RNAs, these structures are believed to support catalytic roles, while the secondary structure of viral RNAs may aid in regulation and in viral packaging. These three types of RNAs possess extensive structures with component units defined by long-range base-pairing interactions. In messenger RNAs, small stem-loop structures are generally involved in regulatory processes, and there is little evidence of the necessity for any large-scale organization in these informational molecules. It would be interesting to see whether RNA secondary structure fractality is correlated in any manner with tertiary conformation, but such an analysis must await structural determinations for medium- and large-sized RNAs.

The fractal dimensions for some natural RNA sequences may reflect a degree of organization incorporated during evolution. There are two alternative mechanisms which may account for the fractal characteristics observed in some RNA secondary structures. One possibility is that broad structural domains were demarcated early in the evolution of RNA, followed by elaboration of smaller, nested structures within these domains. A more probable mechanism, however, involves the initial formation of small hairpin structures, which, through subsequent evolution, were ligated together to form clusters of stem-loop structures. These early domains, which may already have possessed rudimentary functional activity, may have continued to evolve by fusing with other domains to form even larger superdomains.

A recursive process of structural construction incorporating elements of both mechanisms may have constituted

Table 1. Fractal dimensions of RNA secondary structures

RNA species	Length [nts]	Length range [nts]	Fractal dimension	Ref.
ribosomal RNA				
28S rRNA (rat)	4802	8–331	0.78 +/− 0.02	[3]
23S rRNA (*E. coli*)	2904	9–323	0.67 +/− 0.02	[4]
18S rRNA (rat)	1874	11–363	0.56 +/− 0.02	[11]
16S rRNA (*E. coli*)	1542	12–290	0.63 +/− 0.02	[4]
RNAse P				
RNAse P (*E. coli*)	377	9–372	0.76 +/− 0.05	[12]
RNAse P (*B. subtilis*)	401	10–384	0.74 +/− 0.05	[12]
viral genomic RNA				
MS2 phage	3569	18–749	0.88 +/− 0.02	[5]
tobacco ringspot virus (satellite RNA)	359	16–236	0.99 +/− 0.05	[13]
messenger RNA				
rabbit α-globin mRNA	552	8–429	0.58 +/− 0.02	[14]
mouse β-globin mRNA	629	9–368	0.32 +/− 0.02	[15]

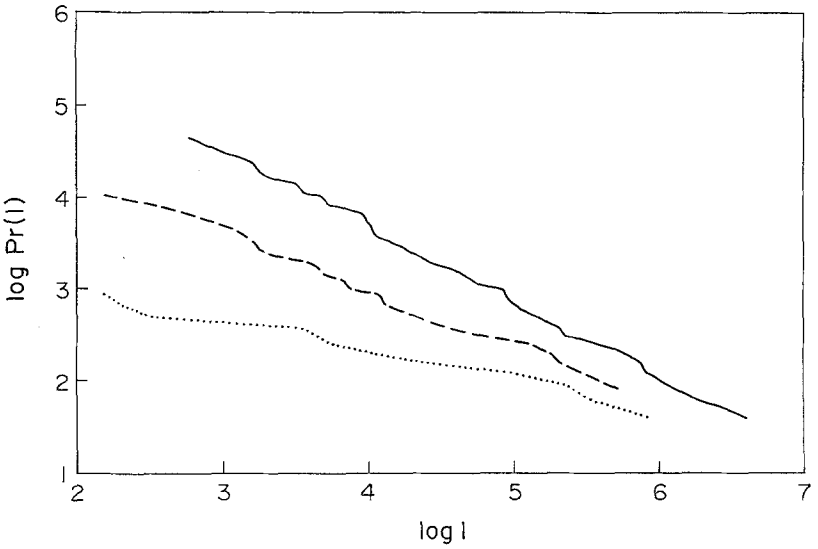

Fig. 2. Logarithmic plots for the structural length distribution $Pr(l)$ for representative RNA molecules. The plots are linear over the length range plotted ($r > 0.97$), with the slopes corresponding to $-d_f$; ——— MS2 phage RNA, – – – rat 16S rRNA, ····· mouse globin mRNA

an early evolutionary fractal cascade that laid the basis for the present-day organization of RNA secondary structure. Theories on the origins and early development of RNA molecules support this hypothesis. There is some speculation, for example, that ribosomal RNAs may have originated from a primitive translation apparatus that consisted primarily of clusters of small hairpin structures [16]. Other RNAs which have catalytic activity, similar to the RNA subunit of RNAse P, may have also formed in this manner in the prebiotic environment. Again, small functional domains may have subsequently evolved to form larger, present-day molecules with distinct, elaborate structures. The fractal organization of RNA secondary structure may be the remnants of this evolutionary process.

Received March 15 and June 22, 1989

1. Zuker, M., Stiegler, P.: Nucl. Acids Res. *9,* 133 (1981); Studnicka, G. M., et al.: ibid. *5,* 3365 (1978)
2. Douthwaite, S., Garrett, R. A.: Biochemistry *20,* 7301 (1981); Ross, A., Brimacombe, R.: Nature *281,* 271 (1979); Kime, M. J., Moore, P. B.: Biochemistry *22,* 2615 (1983)
3. Hadjiolov, A. A., et al.: Nucl. Acids Res. *12,* 3677 (1984)
4. Noller, H. F.: Ann. Rev. Biochem. *53,* 119 (1984)
5. Min Jou, W., et al.: Nature *237,* 82 (1972); Fiers, W., et al.: ibid. *256,* 273 (1975); *260,* 500 (1976)
6. Mandelbrot, B. M., in: The Fractal Geometry of Nature. San Francisco: Freeman 1982
7. Mandelbrot, B. M.: Proc. Nat. Acad. Sci. USA *72,* 3825 (1975)
8. Sander, L. M.: Nature *322,* 789 (1986); Damme, H. V., et al.: ibid. *322,* 731 (1986); Avnir, D., Farin, D.: ibid. *308,* 261 (1984)
9. Lewis, M., Rees, D. C.: Science *230,* 1163 (1985); Wagner, G. C.: J. Am. Chem. Soc. *107,* 5589 (1985)
10. Berger, J. M., Mandelbrot, B.: IBM J. Res. Dev. *7,* 224 (1963)
11. Chan, Y., et al.: J. Biol. Chem. *259,* 224 (1984)
12. James, B. D., et al.: Cell *52,* 19 (1988)
13. Semancik, J. S., in: Viroids and viroid-like pathogens. Boca Raton: CRC Press 1987
14. Heindell, H. C., et al.: Cell *15,* 43 (1978)
15. Lockard, R. E., et al.: Nucl. Acids Res. *14,* 5827 (1986)
16. Clark, C. G.: J. Mol. Evol. *25,* 343 (1987); Kuhn, H., Waser, J.: Nature *298,* 585 (1982)

Naturwissenschaften 76, 473 – 475 (1989)

Is Dimethylsulfonium Propionate an Osmoprotectant of Terrestrial Glycophytes?

A. Chrominski, D. J. Weber, B. N. Smith and D. F. Hegerhorst
Department of Botany and Range Sciences

R. D. Horrocks and K. W. Burgener
Department of Agronomy and Horticulture, Brigham Young University, Provo, UT 84602, USA

Lovelock et al. [1] postulated that dimethylsulfide (DMS) plays a prominent role in global biogenic sulfur transfer from the sea to the air and to the land. One of the major sources of DMS is marine phytoplankton with greater DMS production in higher salinities [2]. Most terrestrial halophytes and facultative halophytes in saline environments apparently produce small amounts of DMS [3]. This study examines DMS production from a terrestrial glycophyte (wheat) not exposed to salt stress but to drought stress.

Studies of DMS evolution from marine organisms [4] led to the demonstration that its precursor was dimethylsulfonium propionate (DMSP) [5]. Consequently, occurrence and possible function(s) of DMSP in marine, littoral plants and in inland halophytes, i.e., in plants exposed to a saline environment, became an active area of research.

Bioemission of sulfur in the form of DMS from land plants to global sulfur cycles has been discussed in [6, 7], however, since the early discoveries were done on plants exposed to salinity the contributions of glycophytes have not been addressed. Few reports have pre-